NASA TECHNICAL NOTE

NASA TN D-4748

NASA TN D-4748

RESEARCH ON FIELD-ALIGNED PROPAGATION OF HF RADIOWAVES USING ALOUETTE-2 TOPSIDE SOUNDER DATA AND DIGITAL RAY-TRACING TECHNIQUES

by

Jayaram Ramasastry and Edward J. Walsh
Electronics Research Center

and

John R. Herman
Lowell Technological Institute
Research Foundation

NATIONAL AERONAUTICS AND SPACE ADMINISTRATION • WASHINGTON, D. C. • AUGUST 1968

RESEARCH ON FIELD-ALIGNED PROPAGATION OF HF RADIOWAVES USING ALOUETTE-2 TOPSIDE SOUNDER DATA AND DIGITAL RAY-TRACING TECHNIQUES

By Jayaram Ramasastry and Edward J. Walsh

Electronics Research Center
Cambridge, Mass.

and

John R. Herman

Lowell Technological Institute
Research Foundation
Lowell, Mass.

NATIONAL AERONAUTICS AND SPACE ADMINISTRATION

For sale by the Clearinghouse for Federal Scientific and Technical Information
Springfield, Virginia 22151 – CFSTI price $3.00

RESEARCH ON FIELD-ALIGNED PROPAGATION OF HF RADIOWAVES USING ALOUETTE-2 TOPSIDE SOUNDER DATA AND DIGITAL RAY-TRACING TECHNIQUES*

By Jayaram Ramasastry and Edward J. Walsh
Electronics Research Center
and
John R. Herman
Lowell Technological Institute
Research Foundation

SUMMARY

The first part of this technical note covers the study of guidance of HF radiowaves along field-aligned paths using the topside sounder data from the Alouette 2 satellite. More than 100,000 Alouette 2 ionograms have been used in this analysis and an unusually high percentage of occurrence of conjugate echoes has been observed in the data of some equatorial stations. The maximum percentage of occurrence of conjugate traces around local midnight when the satellite is near the apogee (3000 km) throws some light on the diffusion mechanism responsible for the formation of field-aligned irregularities. The Singapore data (Geomagnetic longitude $180^{\circ} \pm 30^{\circ}$) has shown higher occurrence of ducted echo-traces (>10 percent) than the data from all other stations. This is rather a large percentage. The longitudinal preference may be conducted with the larger magnetic field strengths in that longitudinal range. Two interesting types of ionograms containing conjugate echo traces are presented. They are called the "double hook" and the "triple hook" types. A self-consistent explanation based on the assumption of multiple reflections between conjugate points of the field line passing through the satellite is presented.

The second part of the note covers the results of the digital ray-tracing study of the guidance of HF radiowaves along field-aligned ionization irregularities in the magnetosphere of the Earth. Various computer results are shown to illustrate the mechanism of guidance of radiowaves. Time-delay and trapping characteristics of the two types of conjugate echoes that are frequently observed in the Alouette 2 topside sounder records are simulated using the ray-tracing methods. Some of the optimum conditions for guidance of electromagnetic waves along a magnetic field line are discussed. The results reported here on the HF ducting phenomenon is directed primarily towards determining whether such a mechanism may be utilized to study the magnetospheric phenomena and whether it can be useful as a reliable communication link.

---

*The information in Part I of this report is also contained in a paper entitled "Field-Aligned Propagation HF Radiowaves Using Alouette-2 Topside Sounder Data," by J. Ramasastry, E. J. Walsh, and J. R. Herman; and the material in Part II is contained in a paper entitled "Field-Aligned Propagation HF Radiowaves Using Digital Ray-Tracing Techniques," by J. Ramasastry, E. J. Walsh, and J. R. Herman. Both of the papers were presented at the AGARD Meeting, August 19-23, 1968, in Oslo, Norway.

PART I

CONJUGATE ECHOES IN ALOUETTE-2 TOPSIDE SOUNDER DATA

Introduction

High frequency conjugate echoes were first observed on the Alouette 1 sweep frequency topside sounder data (ref. 1). Conjugate signals have also been observed on the Explorer 20 fixed-frequency topside sounder ionograms (ref. 2). Some occurrence statistics concerning the Alouette 2 ionograms have also been published (ref. 3). However, the study of HF conjugate echoes on Alouette 2 ionograms has offered challenging problems and some exciting results. Two types of ionograms containing symmetric conjugate echo traces which appear frequently are presented and explained in terms of multiple reflections between the conjugate points of a field line passing through the satellite. Such symmetric traces have not been previously reported in the literature.

The Alouette 2 topside sounder is better suited to the study of conjugate echoes than that of Alouette 1 because of the lower frequency limit of the sounder. The transmitter and the receiver are tuned to the same frequency which is swept in time. The transmitter is pulsed once in 32 msec and the instrumentation provides a new zero time-reference each 32 msec, thus pulses returning with delays of 37, 69, or 101 msec will all be recorded as traces of 5 msec group-delay on the same ionogram frame. More than 100,000 ionograms from eight stations (Quito, Fort Myers, Santiago, Johannesburg, Kano, Singapore, Winkfield, and Orroral Valley) have been examined by the authors and some of the observations of the HF ducting phenomena in the magnetosphere of the Earth have been very revealing. Various statistical results are presented and the occurrence characteristics of the conjugate echoes are discussed.

Method of Analysis

All the available ionograms from the eight stations were analyzed to identify the ionograms with conjugate traces. Muldrew (ref. 3) classified all the available ionograms into five groups depending on the value of f_{xs}, the frequency of the extraordinary wave which has zero refractive index at the satellite altitude. The reason given by the author for such a classification is that it gives a rough indication of the electron density at the satellite altitude. While it is a convenient method of classification, it does not provide any new physical insight into the guidance of HF radiowaves. Consequently, the

authors have not adopted any method of classification of frames with conjugate echoes. The statistical data in the present analysis are restricted to those ionograms which exhibit conjugate echoes. Hence the percentage occurrence should be taken to mean that so many out of 100 ionograms with conjugate ducts occur at the indicated value of the parameter (altitude, local-time, or L-value).

Since the argument that the perigee rotates only 1.89 deg/day, which is almost the same as the precession of the orbital plane with respect to the sun, the local time at perigee (or apogee) changes less than 3 hr/yr. For the period of the data used in our analysis, the perigee occurs near local noon and the apogee near local midnight. Hence the satellite intersects the smaller L shells near noon and the larger L shells near midnight. As we shall see later, the percentage occurrence is rather large around local midnight when the satellite is near the apogee.

Conjugate Echoes as a Function of L Value

The percentage occurrence of conjugate echoes between 21 hours and 04 hours local time is plotted as a function of L in Figure 1. This period of local time is chosen to afford comparison with the results of Muldrew (ref. 3). The results presented here are consistent with Muldrew's argument that the occurrence percentage is high and almost constant during this time period. The results for L values larger than 3.5 are not considered representative and hence may be deleted from discussion. Very few conjugate ducts are observed at these high L values because the receiver is no longer tuned to the frequency of echoes that arrive after the long delay required for propagation along a duct with an L value about 4 or greater. Such a conclusion agrees with our analysis of "triple hook" and "double hook" traces where the traces corresponding to multiple reflections between the conjugate point start fading out as the group delay exceeds 200 msec. The authors' results also show an apparent drop in occurrence for L less than about 1.35. It can also be agreed that such a rapid drop may not be real since the data at such low L values are not representative because of the characteristics of the satellite orbit, i.e., the satellite intersects lower L shells during local noon where the percentage occurrence of conjugate echoes is almost zero (ref. 3). One may say in this context that the Alouette 2 satellite was not designed originally to study conjugate ducting. Future experiments designed to study conjugate ducting should have the capability of receiving signals for longer periods of time at any one frequency; in addition, the orbital characteristics of the satellite should be such that the data are representative of guidance in field lines of both low- and high-L values.

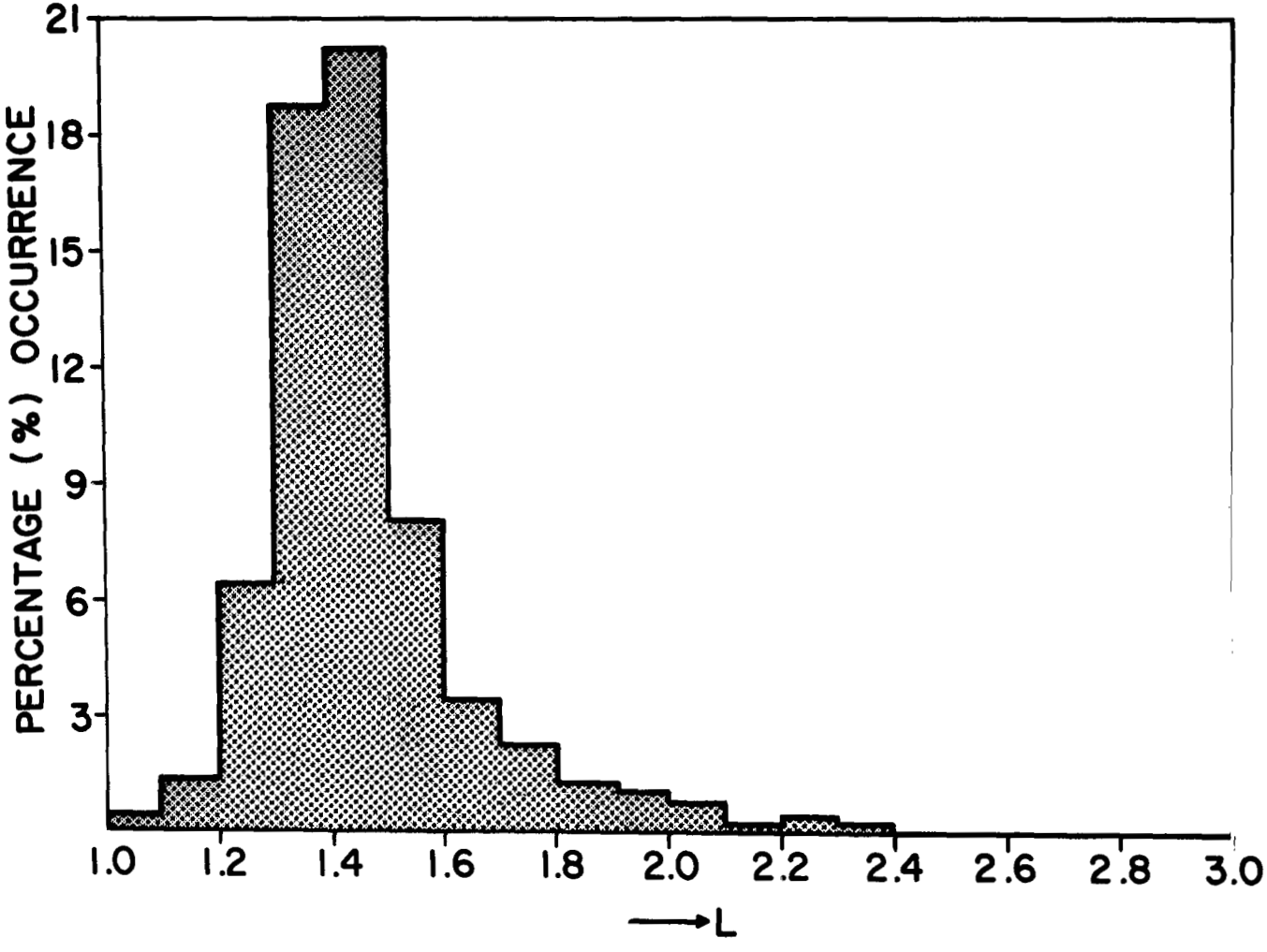

Figure 1.- Percentage occurrence of conjugate ducts as a function of L value

Conjugate Echoes as a Function of Local Time (1-hour averages)

The percentage occurrence of conjugate echoes as a function of local time is shown in Figure 2. The data were averaged in 1-hour intervals of local time. This averaging time interval is selected in view of the fact that the local time drift along the propagation path may be about an hour. It can be seen that the percentage occurrence of conjugate echoes is almost zero in the time interval 0600 to 1800 hours local time. There is a pronounced broad maximum between 2100 and 0400 hours local time. The post-midnight maximum in duct occurrence when the satellite altitude is near apogee brings forth the discrete characteristics of the field-aligned ionization irregularities. As may be noted, the ambient density during night time is considerably lower and any diffusion mechanism capable of channelling the particles along the field line creates larger gradients of electron density along the field line during the night time. Hence the increased efficiency in the guidance of radiowaves during night time can be anticipated.

Conjugate Echoes as a Function of Satellite Altitude

The percentage occurrence of conjugate echoes as a function of satellite altitude is shown in Figure 3. As mentioned before, the satellite is around the midnight meridian when it approaches the apogee of its orbit. Hence the high altitude maximum is consistent with the previous conclusions about midnight maximum. Conjugate echoes are rarely seen at altitudes less than 1200 km in the Alouette 2 data.

Examination of Conjugate Traces

In the Alouette 2 ionograms, the conjugate echoes generally appear as beautifully symmetric patterns of high intensity. When they appear, the normal traces in the ionogram are faded out because of the automatic gain control in the receiver. Figure 4 shows a series of evenly spaced "double hooks" separated by horizontal traces, while Figure 5 shows a pattern of symmetric "triple hooks." The symmetry of these patterns is in sharp contrast to the types of conjugate traces reported by Muldrew (ref. 1) for Alouette 1 data. They are also in sharp contrast to the conjugate traces reported by Muldrew (ref. 3) for Alouette 2 data. The L values of the magnetic field lines passing through the satellite for these two examples (L = 1.53, 1.63, respectively) are larger than the L values for the conjugate echo traces

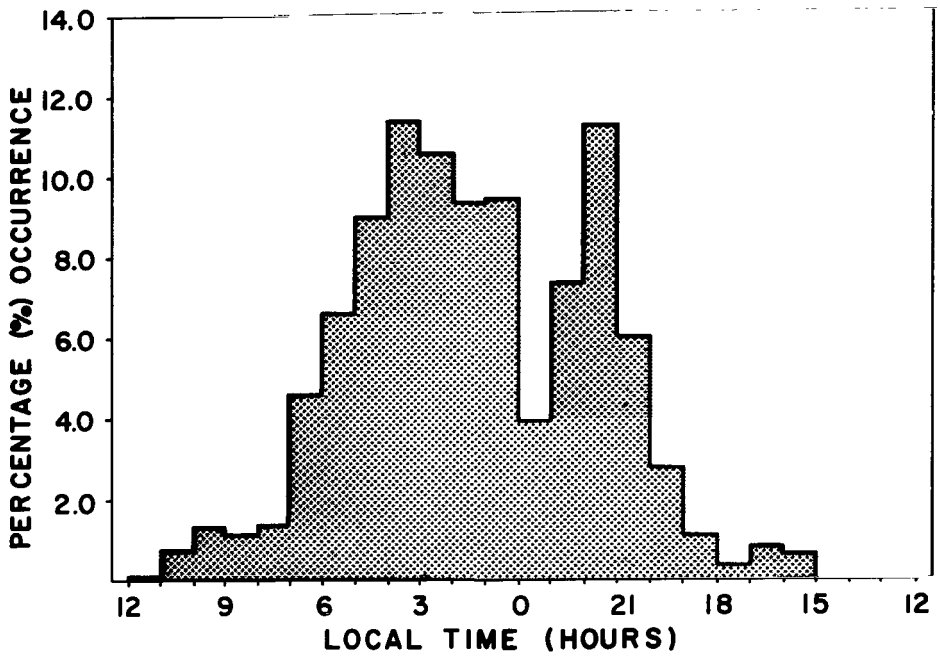

Figure 2.- Percentage occurrence of conjugate ducts as a function of Local Time (1-hour average)

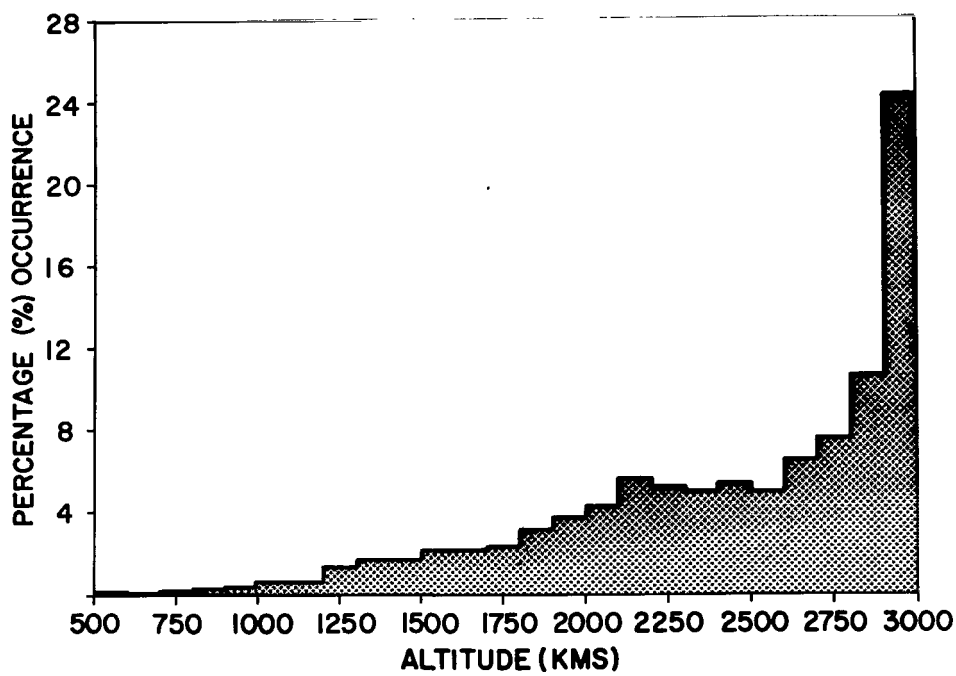

Figure 3.- Percentage occurrence of conjugate ducts as a function of altitude (100-km average)

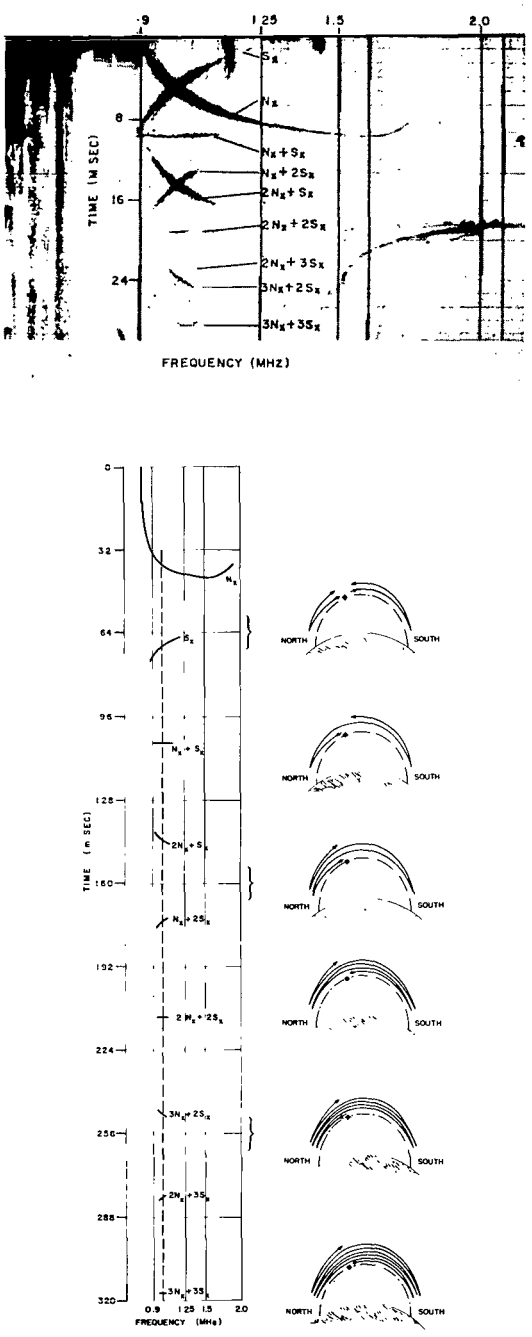

Figure 4. - The "double hook" pattern recorded at Quito, Ecuador, on Aug. 18, 1966, at 08:00:05 GMT. (Local Time = 02:07:46, Geomag. Lat. = 12.56°N, Geomag. Long. = 18:22°W, L = 1.53)

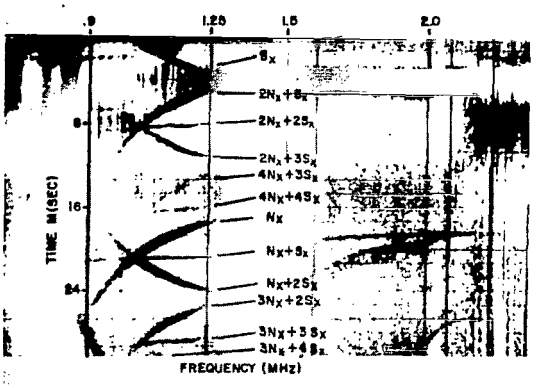

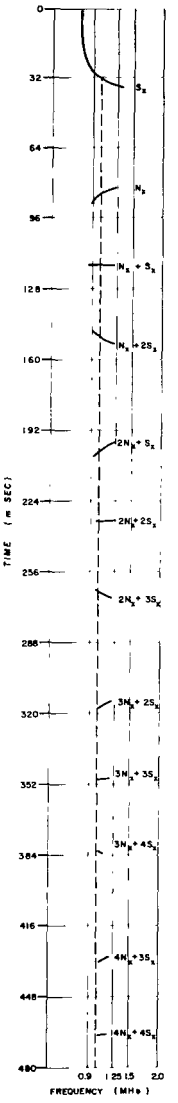

Figure 5. - The "triple hook" pattern recorded at Santiago, Chile, on April 22, 1966, at 09:01:48 GMT. (Local Time = 04:38:41, Geomag. Lat. = 19.53°S, Geomag. Long. = 2.54°E, L = 1.63)

considered by Muldrew (ref. 1) for the Alouette 1 data. Hence, the major portions of the paths are in the regions of low electron densities for the cases considered here. This means that the group delay for a round trip path (N + S) should be relatively independent of frequency and approximately determined by the geometrical length of the field line between the two conjugate reflection points. N and S correspond to the north and south directions taken by the signal. Only the extraordinary wave traces of conjugate echoes are observed. Hence all the round trip traces (N + S, 2N + 2S, 3N + 3S,...) should have a tendency to appear as horizontal lines in the ionograms. The symmetry of the "double hook" and "triple hook" patterns follows directly from this characteristic. The far end echo from the satellite always heads along the field line away from the Earth towards the region of decreasing electron density, except at the equator where the path-lengths and the characteristics are the same. Hence, reflections were not obtained from near the satellite as for the case of the near-end echo which follows the field line towards the Earth and towards the region of increasing electron density. This results in reflections from near the satellite. The subsequent symmetry of the N and S traces follows from the magneto-ionic properties of the ray path.

The ionogram in Figure 4 is a typical example of the frequently observed "double hook" patterns. It was recorded at Quito, Ecuador. Also shown in the figure are the proper relative positions of the various traces according to their actual time delays. The satellite position (GM Lat = 12.56^{o}) is such that the group-delays of the near-end and far-end paths along the field line differ approximately by 32 msec and the North and South traces seem to intersect in real time. The geometry of the path length of the field line requires the round trip trace (N + S) to be positioned twice as far from the beginning of its own time frame as the apparent intersection point of the N and S traces. The (2N + 2S) trace should be twice as far from the beginning of its frame as the (N + S) trace is from the beginning of its own time frame. Similar geometric considerations can account for the uniform spacing of the traces in the ionogram. The (2N + S) and (3N + 2S) traces are shaped like the N trace, and the (N +2S) and (2N + 3S) traces are shaped like the S trace. This is because the delay times for the round trip traces (N + S), (2N + 2S), (3N + 3S),... are virtually independent of frequency. The direct consequence of such a situation is that all the "double hook" traces do have the same shape. The (3N + 3S) trace is extremely faint but is discernible on the microfilm.

Figure 5 shows the "triple hook" ionogram and its various characteristics. The reason that all the triple hooks in the ionogram of Figure 5 have the same shape is once again caused by the frequency-independent group-delay characteristics of the

round trip traces. The figure also shows the various traces according to their respective time delays. The near-end trace is easily recognizable in both Figures 4 and 5 because it is the most intense trace which starts from zero group delay. This characteristic is caused by reflections from near the satellite due to the increasing electron density in that direction. In both the ionograms, the far end trace was initially selected on the basis of its intensity and the mirror-image-like characteristic with respect to the near-end trace. Also, the L value of the field line corresponding to that frame gave the clue as to the approximate group-delay of the far-end echo. Digital ray tracing analyses have, since then, borne out these assumptions.

Figure 5 exhibits triple hooks instead of double hooks because the satellite is displaced from the magnetic equator (GM Lat = -19.53°) so that the group-delays of the near-end and far-end echo traces differ by more than 32 msec. The apexes of all the triple hooks occur at the frequency where the time delay of the near end (S) echo is exactly one frame time (32 msec). Then the N, N + S, and N + 2S echoes all have the same positions in their relative time frames at that frequency and will seem to intersect in the ionogram where all the time frames are superimposed.

There is one significant condition which determines whether the conjugate echoes form a triple hook pattern or a double hook pattern. Double hooks are observed when the group-delays of the near-end and far-end echoes differ by approximately 32 msec. Triple hooks are observed when the group-delays differ by more than 32 msec.

The traces representing the round trip paths are sometimes inclined to the horizontal. The slopes of (2N + 2S), (3N + 3S), (4N + 4S), and so forth, are exactly twice, thrice, four times, and so forth, the slope of the trace (N + S). This can be easily verified by adding up the various group delays. Such inclined round-trip traces appear when the near-end and far-end distances differ by a small amount.

One of the significant features observed in Figure 5 is that the (4N + 4S) trace had a delay time of 465 msec. But with the receiver bandwidth of 30 kHz and the sounder frequency-sweep rate of 0.15 MHz/sec, the receiver is essentially detuned after 200 msec. This may mean that the faintness of the (4N + 4S) trace is not caused by the leakage and attenuation of the signal within the "magnetospheric wave-guide." On the contrary, the signal after transversing four complete round trips from one hemisphere to the other, covering a total path-lenght of about 60,000 km, must have been quite strong to have shown up at all in the detuned receiver.

The faint (3N + 3S) trace in the "double hook" case (Figure 4) has a time delay of 316 msec and probably would have been more intense if the receiver had been properly tuned to receive it.

Figure 6 shows a conjugate echo frame corresponding to a high L value of 1.76. The satellite was at -19.05° (mag. lat.) and the total field-aligned path was 17,463 km with the near-end and far-end distances being 6593 and 10,870 km, respectively.

Figure 7 shows a series of seven ionograms recorded at Quito on June 12, 1966, from 03:23:45 to 03:26:59 UT. As may be seen the triple hooks prominently appear and disappear. Such a sequence is representative of an event when the satellite passes through a cluster of ionization irregularities with strong coupling of signals into ducts of various closely spaced L shells.

One may also emphasize in this context that the ionization irregularities transverse to the field lines responsible for such a wave guidance may be either enhanced or depleted columns of ionization. The nature of the irregularities is not discussed in the present note.

Discussion and Conclusion

One must bear in mind that the Alouette 2 satellite topside sounder experiment was not originally designed for detecting such long time-delay echoes. The frequency sweep rates and bandwidths used are essentially sufficient to receive the signals normally incident on the topside ionosphere. The Explorer 20 satellite (ref. 2) had a fixed frequency topside sounder transmitting at seven different frequencies in sequence, each time the corresponding receiver being tuned for 15 msec. The next time the receiver could receive the signal at that frequency was 105 msec later. Since the satellite altitude was only 1000 km (circular orbit) like that of Alouette 1, the experiment was once again not suitable for the study of conjugate ducting. A suitably designed satellite propagation experiment, with its receiver being capable of receiving signals of larger time delays, may unravel all the mysteries about magnetospheric wave-guidance.

The authors also propose an experiment in which a transmitter in a low orbiting satellite (preferably eccentric polar orbit) transmits at HF to a high-altitude satellite (altitude of apogee ~6000 km) whose receiver should have the capability of receiving the signals for longer periods of time. The now orbiting Radio Astronomy Satellite might have the desired receiving characteristics in the frequency range 1-10 MHz. Many monostatic and bistatic radar experiments of the past aimed at

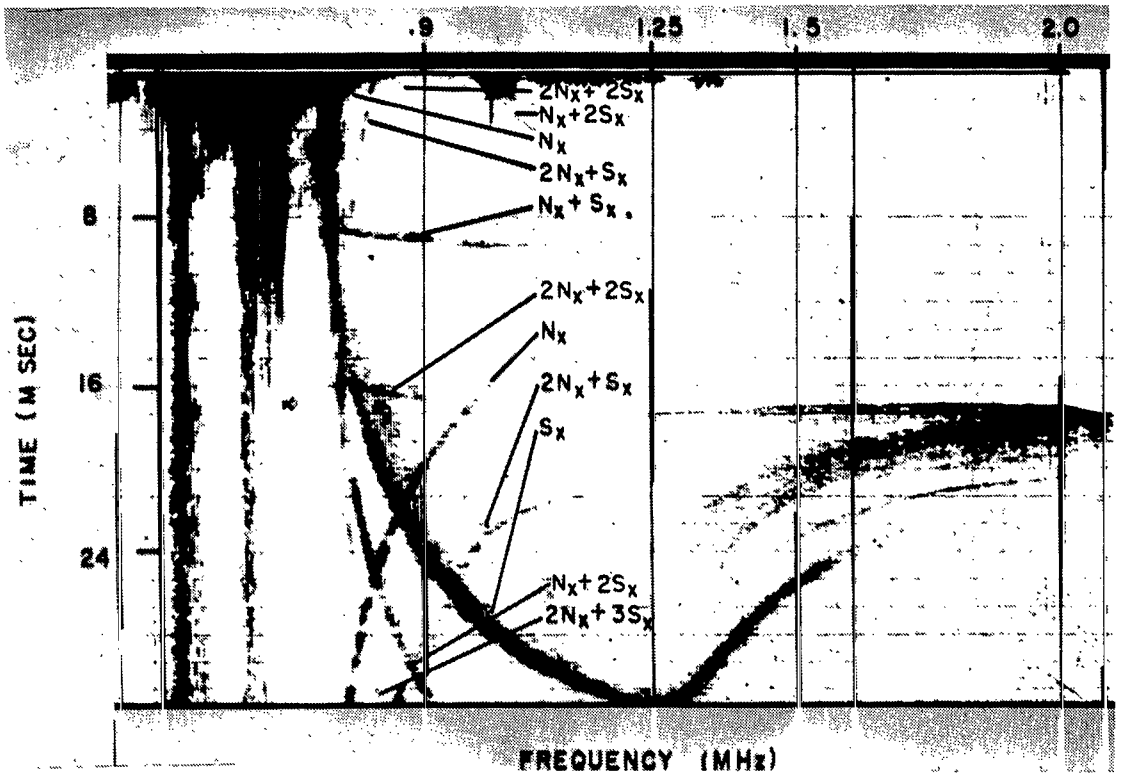

Figure 6. - Ionogram showing conjugate echoes for a high L value (L = 1.76) recorded at Johannesburg, South Africa, on Aug. 12, 1966, at 02:02:54 GMT. (Local Time = 02:37:05, Geomag. Lat. = -19.05°S, Geomag. Long. = 74.53°E)

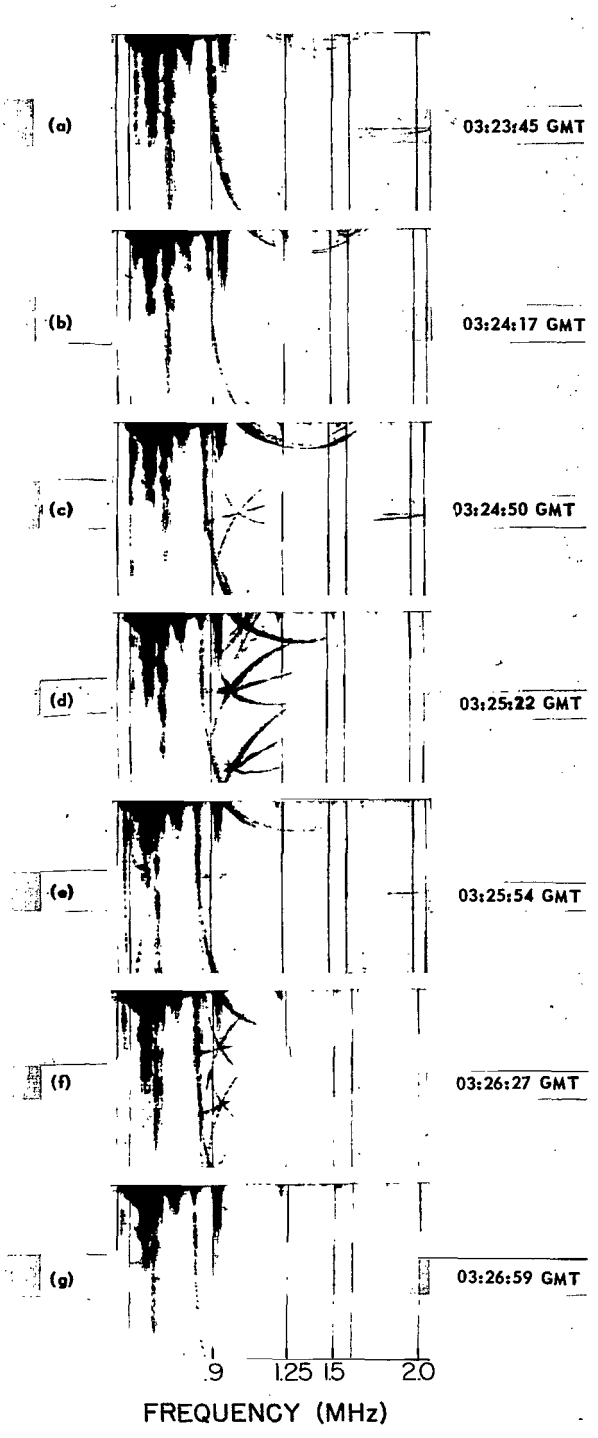

Figure 7. - A series of seven ionograms recorded at Quito, Ecuador, on June 12, 1966, from 03:23:45 to 03:26:59 GMT.

verifying the existence of ducts and shells in the magnetosphere and the consequent guidance of electromagnetic waves have been inconclusive. The stability and frequency of occurrence of the conjugate echoes combined with the relatively loss-free multiple reflections between the conjugate points, of the signals observed in the Alouette 2 satellite data have created challenging opportunities. Thus a well designed experiment may provide conclusive answers to the question of whether or not this unique magnetospheric wave guide could be used as a reliable HF communication link between conjugate points or between two satellites over large transequatorial distances along a field-aligned path. Even if this propagation mode cannot be used as a communication link, its use to study the magnetospheric phenomena cannot be discounted.

PART II

DIGITAL RAY-TRACING STUDIES

Introduction

Some of the echo traces appearing at virtual ranges greater than those of the normal vertical incidence echo traces on the topside sounder ionograms have been explained in terms of field-aligned ionization irregularities (ref. 1). The irregularities are assumed to have thicknesses greater than the radio wavelength and to act as waveguides or "ducts" to trap HF energy and produce the long-range echo traces. A complete review of the past theoretical and experimental work directed towards testing such a guidance mechanism has been published (ref. 4).

The guiding of rays along field lines requires irregularities with a certain minimum transverse ionization gradient. Propagation between magnetic conjugate points or "conjugate ducting" occurs when the transverse ionization gradient exceeds the minimum required for guidance at the apex of the magnetic line of force. The current interest in the HF ducting phenomenon is directed primarily towards determining whether such a mechanism may be utilized to study the megnetospheric phenomena and whether it can be useful as a reliable communication link. Here, we also examine the conditions under which the HF radiowaves may be guided along field-aligned ionization irregularities.

Ray-Tracing Method

The ray tracing method is based on Hamilton's system of equations (ref. 5) as derived in spherical polar coordinate system by Haselgrove (ref. 6) and extended by Grossi and Langworthy (ref. 7) for the investigation of HF and VHF ionospheric progagation. The reader is referred to reference 7 for a description of the basic ray-tracing program. Because of the high accuracy obtainable, the use of a high-speed digital computer is preferred to an analog machine for the integration of the ray equations. The Adams-Moulton variable step-size integration method (ref. 8) is adopted because of its greater flexibility due to an automatic error control which halves or doubles the step size to ensure the desired accuracy along all parts of the ray path.

Magnetospheric Models

The electromagnetic properties of the magnetosphere are characterized by (1) the electron density distribution, (2) the

magnetic field distribution, and (3) the electron collision-frequency distribution. The mathematical models for the above three items are implemented in the form of subroutines and can therefore be modified as and when necessary.

Magnetic Field Model

To a first approximation, a dipole model is used for the magnetic field of the Earth. The magnetic field equation which defines the gyrofrequency f_H is given by:

$$f_H(r,\theta) = C_{11}\left(\frac{a}{r}\right)^3 \sqrt{1 + 3\cos^2 \theta} \qquad (1)$$

where a is the radius of the Earth, and r and θ are the geocentric distance and colatitude of any point on the field line.

$$C_{11} = \frac{e}{2\pi m} B_o \times 10^{-6} \approx 0.9 \qquad (2)$$

where B_o is the magnetic field on the surface of the Earth at the equator, and e and m are the charge and mass of an electron. A value of 0.3142 gauss is used for B_o.

For ray tracing along high L-value field lines, the 63-term spherical harmonic expansion of Cains, Daniels, Hendriks, and Jensen (ref. 9) is used.

Collision Frequency Model

The collision frequency model is based on results published by F.S. Johnson in the Satellite Environment Handbook (ref. 10).

Electron Density Model

The model for the electron density distribution incorporates those features that have a bearing on the high-frequency ducting problem. Thus, an ionization irregularity normal to the field line is superimposed on the normal radial distribution of electron density. In this model, the electron density is given by:

$$N(r,\theta,\phi) = N_1(r,\theta) * N_2(r,\theta,\phi) \qquad (3)$$

where θ is the colatitude and ϕ is the magnetic longitude. $N_1(r,\theta)$ represents the background density in the magnetic meridional plane and $N_2(r,\theta,\phi)$ represents the ionization in the field-aligned irregularities in both the meridional and azimuthal planes.

The background ionization is assumed to have the form:

$$N_1(r,\theta) = N_F + N_X \ . \tag{4}$$

Here N_F and N_X refer to the electron densities in the ionospheric F-region and the exosphere, respectively.

$$N_F = N_{max} * \exp\left[\frac{1}{2}\left\{1 - W - e^{-W}\right\}\right] \tag{5}$$

where N_{max} is the peak electron density and

$$W = \frac{h - h_{max}}{H_F} \tag{6}$$

in which h_{max} is the altitude of the peak electron density, N_{max} and H_F is the scale height. In our calculations, the maximum altitude h_{max} is assumed to be 350 km and H_F = 50 km.

The Angerami and Thomas diffusive equilibrium model (ref. 11) is used for the exospheric electron density distribution above 1000 km and below the plasma-pause which exists at a distance of from 3 to 4.5 Earth radii. The centrifugal force caused by the rotation of the Earth is neglected, while applying the Angerami and Thomas model. With this model, the electron density in the exosphere is given by:

$$N_X = N_r * \left[1.659 \times 10^{-3}\theta + 1.662 \times 10^{4}\right] \tag{7}$$

where θ is the colatitude in degrees. The terms within the brackets represent the latitudinal variation of exospheric electron density as derived by Thomas and Sadar (ref. 12) using Alouette 1 satellite data.

$$N_r(Z) = \left[\sum_i \beta_i \exp\left[- \frac{Z_X}{H_i} \right] \right]^{\frac{1}{2}} \tag{8}$$

where Z_X is the geopotential altitude given by

$$Z_X = \frac{r_o}{r}(r - r_o) \tag{9}$$

where r_o is the reference radial distance and is equal to 6870 km in the model. The symbol i refers to each ion present in the exosphere. H_i and β_i refer to the scale height and the fractional density of the i^{th} ion at the reference level r_o. The scale height is given by

$$H_i = \frac{kT_i}{M_i g(r_o)} \tag{10}$$

where k is the Boltzmann Constant, T_i and M_i are the temperature and mass, respectively, of the i^{th} ion, and $g(r_o)$ is the acceleration due to gravity at the reference level r_o. A three-ion gas model consisting of oxygen (O^+), helium (He^+), and Hydrogen (H^+) ions is assumed. The various parameters in the density equation have the following values:

$$T = 1000^{o}K \quad \text{for both electrons and ions} \tag{11a}$$

$$\beta_{He} = \frac{0.2 \times 10^{-T/1000}}{\beta_e} = 1.96 \times 10^{-2} \tag{11b}$$

$$\beta_H = \frac{0.16 \times 10^{-T/500}}{\beta_e} = 1.6 \times 10^{-3} \tag{11c}$$

$$\beta_O = \frac{1}{\beta_e} = 0.9788 \tag{11d}$$

$$\beta_e = 1 + 0.2 \times 10^{(-T/1000)} + 0.16 \times 10^{(-T/500)}$$

$$= 1.0216 \qquad (11e)$$

The technique suggested by Swayze (ref. 13) is used to join the exospheric profile smoothly with that of the F-layer between 350 and 1000 km. The expression for N_x is modulated by a factor

$$\exp\left[-\left(\frac{h - 1000}{500}\right)^2\right] \qquad (12)$$

where h is the altitude in kilometers.

The electron density as a function of altitude at various geomagnetic latitudes is shown in Figure 8.

Model for the Ionization Irregularities

The following assumptions are made in the development of this model:

1. The ionization in the irregularities is distributed in discrete columns or sheets separated in latitude and aligned with the magnetic field lines.

2. The transverse scale of the field aligned irregularities follows the transverse (meridional) dimensions of the tube of magnetic flux.

3. The peak enhancement varies inversely as the transverse dimensions of the tube of magnetic flux.

4. The variation of the density within the irregularity follows a Gaussian distribution transverse to the magnetic field. The Gaussian distribution satisfies the equations for the diffusion of charged particles across a field line.

Hence:

$$N_2(r,\theta) = 1 + \frac{\Delta N_o}{N^*\left(\frac{t}{t_o}\right)} * \exp\left[-\left(\frac{\Delta Z}{\frac{t}{t_o} H_o}\right)^2\right] \qquad (13)$$

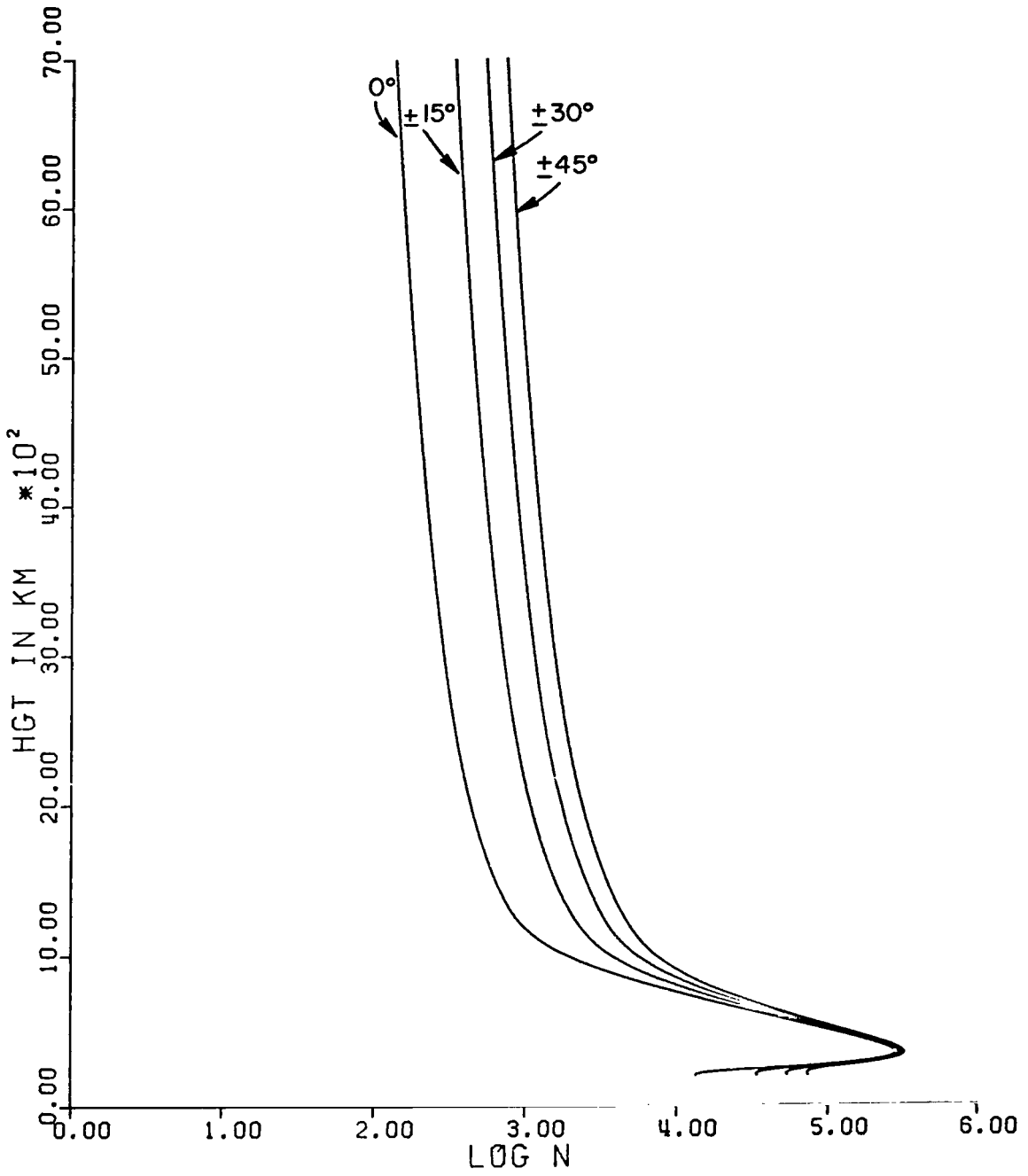

Figure 8. - Electron density (cm^{-3}) versus altitude profile for geomagnetic latitude of 0°, ±15°, ±30°, ±45°

N_o is the peak ionization enhancement and H_o is the scale size of the irregularity at the base of the field line.

$$\frac{t}{t_o} = \frac{\text{Meridional width at } (r,\theta)}{\text{Meridional width at } (r_o,\theta_o)}$$

$$= \frac{\sin^3 \theta (4 - 3\sin^2 \theta_o)^{\frac{1}{2}}}{\sin^3 \theta_o (4 - 3\sin^2 \theta)^{\frac{1}{2}}} \qquad (14)$$

While specifying the initial coordinates of the starting point, the geographic latitude, λ_a, and the longitude, ϕ_a, are converted to geomagnetic coordinates λ_m and ϕ_m by using the following transformation equations:

$$\tan \lambda_m = -\tan(\lambda_a - \lambda_o)\sin x \sec (x + \phi_o) \qquad (15)$$

$$\tan \phi_m = -\cos \lambda_m \tan (x + \phi_o) \qquad (16)$$

where

$$x = \arctan\left\{\cos (\lambda_a - \lambda_o)\cot \phi_a\right\} \qquad (17)$$

and

$$\phi_o = +78.5^o \quad \text{and} \quad \lambda_o = +291.0^o$$

are the geographic coordinates of the geomagnetic pole.

RESULTS

Figures 9 through 13 show a few results of the ray tracing. Figures 9 through 12 simulate some of the conjugate echo paths observed in Alouette 2 ionograms. Parameters shown in the figures are defined as follows:

R_o = the geocentric distance (km) of the initial signal position,

PKFRAC = the peak fractional ionization enhancement,

LAMBDA = the colatitude of the field line,

A_o = the initial angle the ray makes with the local vertical,

B_o = the initial angle the ray makes with the South vector,

PHI and THETA = the magnetic longitude and colatitude of the initial signal position.

The frequency of the signal is 1.0 MHz for the cases considered in Figures 9 through 12.

Each figure consists of two plots. The rectangular plot shows the distance of the ray from the field line versus the distance along the field line from the near end. The polar plot shows the actual ray path with reference to the surface of the Earth. The polar plots gives a clear indication of the positions of the conjugate reflection points as well as the L value of the field line guiding the rays.

Figure 9 shows the L = 1.76 case using a peak electron density enhancement of 13.0 percent at the point the ray is launched. A peak enhancement of 13.0 percent at a geocentric distance of 10,022 km corresponds to a much smaller percentage at lower altitudes. The ray starts at about 12,500 km along the field line from the northern hemisphere. It gets reflected on its way towards the Earth and travels all the way back to the southern hemisphere where it is reflected again. The program was stopped deliberately when the ray was at 15,500 km along the field line. Otherwise, it could have bounced back and forth indefinitely. The bowing of the pattern at the equator is caused by larger scale sizes near the equator so that the ray rides further out from the field line because the enhancement structure is wider.

The oscillatory nature of the ray path seen in the rectangular plot is caused by the ray being launched too far away

where the electron density gradient is insufficient to bend the ray back towards the direction parallel to the field line. The ray essentially tends to continue in a straight line, but appears to fall in towards the field line since the field line is curved. When the ray gets close enough, the gradient is large enough to bend the ray away from the field line and the apparent inward motion stops in the rectangular plot. It follows that similar oscillations also occur if the ray is launched too close to the field line or at the wrong angle relative to its equilibrium position. A careful launching of the signal can eliminate all these initial oscillations even though they may grow later when the ray crosses the equator or upon reflection.

In Figures 10 and 11, the rectangular plots show one reflection each for the cases L = 1.63 and L = 1.53, respectively, while the corresponding polar plots show several round trips. For these two cases, the peak enhancement is 6 percent at the point of launch.

Figure 12 shows how a small peak enhancement is sufficient (3.0 percent) to trap the rays if the signal is properly launched. The physical conditions are the same as for the case of Figure 9.

Figure 13 relates to an L = 2 field line and shows the manner in which a ray typically escapes when the oscillations grow too large, even with sufficient peak enhancement. A frequency of 2.00 MHz is used for this case.

National Aeronautics and Space Administration
Electronics Research Center
Cambridge, Massachusetts, July 1968
188-39-01-01

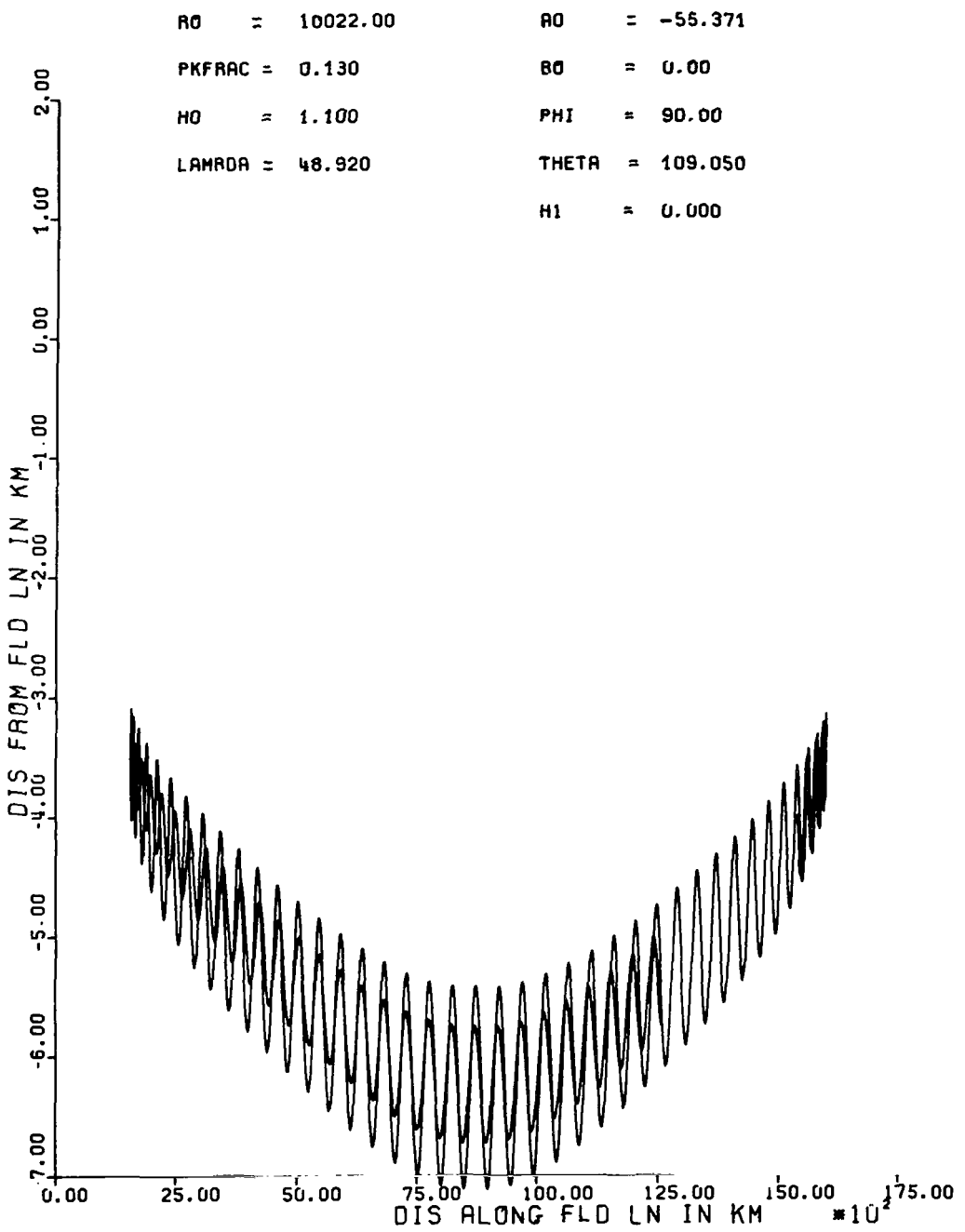

Figure 9. - Ray tracing showing multiple reflections along the L = 1.76 field line for 13.0 percent peak enhancement of electron density at a geocentric distance 10,022.00 km (frequency = 1 MHz, extraordinary wave)

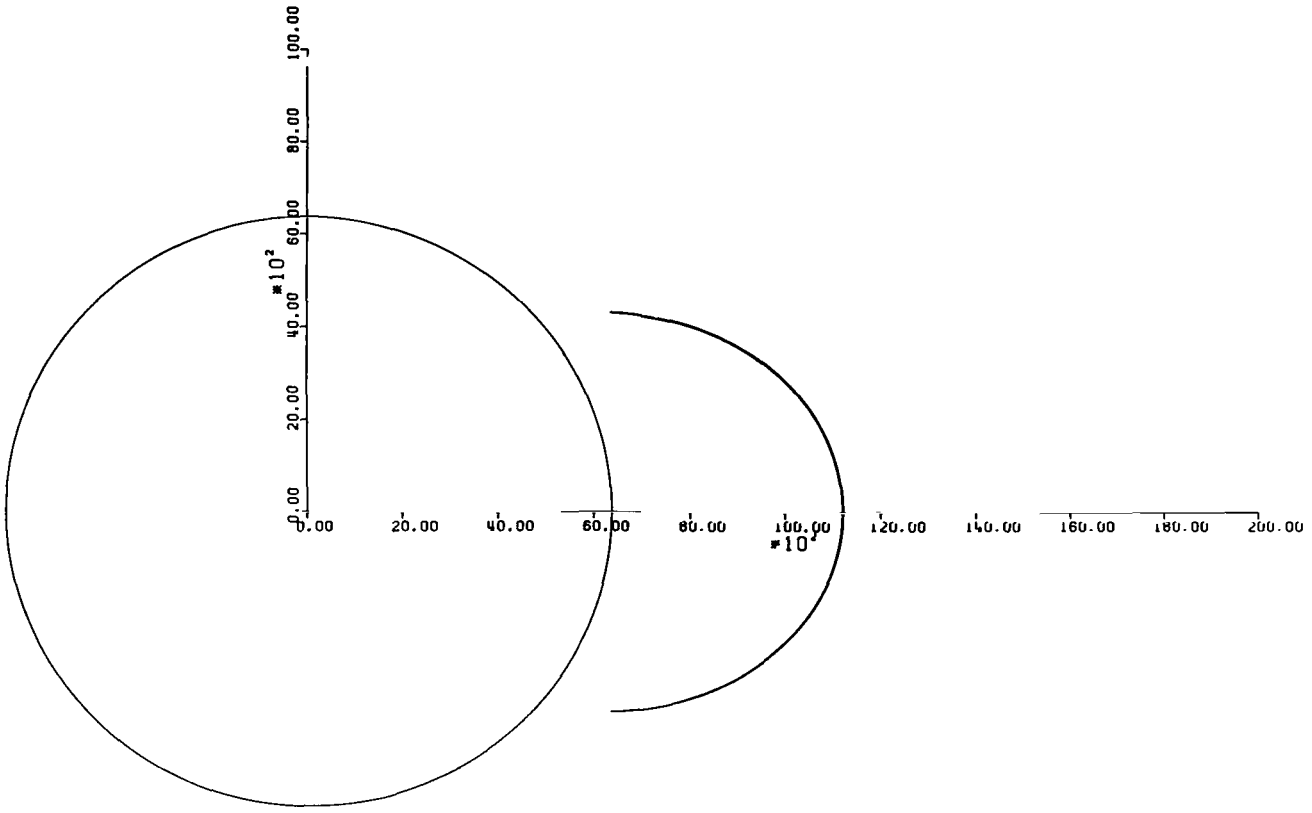

Figure 9. (Concl'd.)

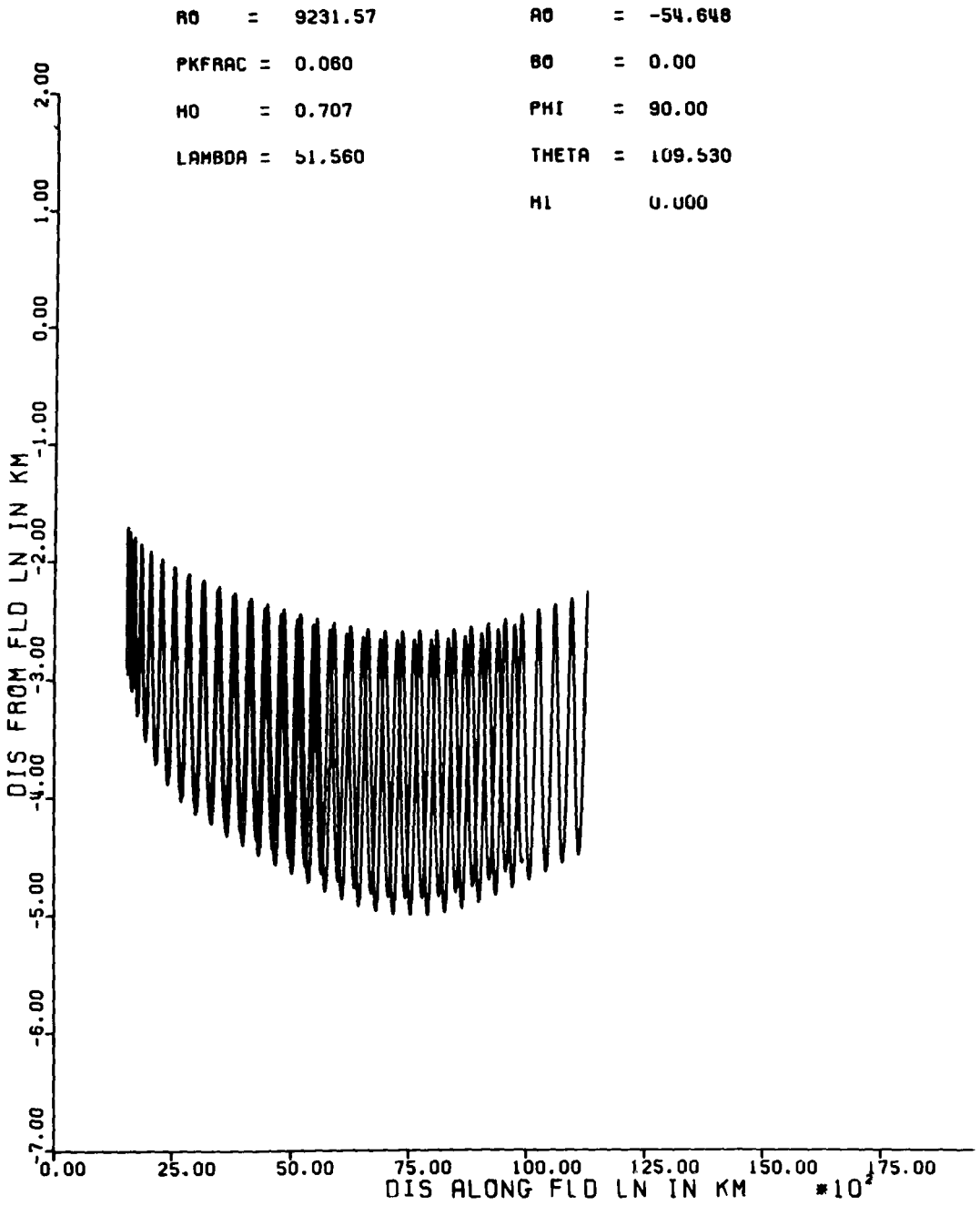

Figure 10. - Ray tracing along the L = 1.63 field-line for 6.0 percent peak enhancement at a geocentric distance of 9231.57 km (frequency = 1 MHz, extraordinary wave)

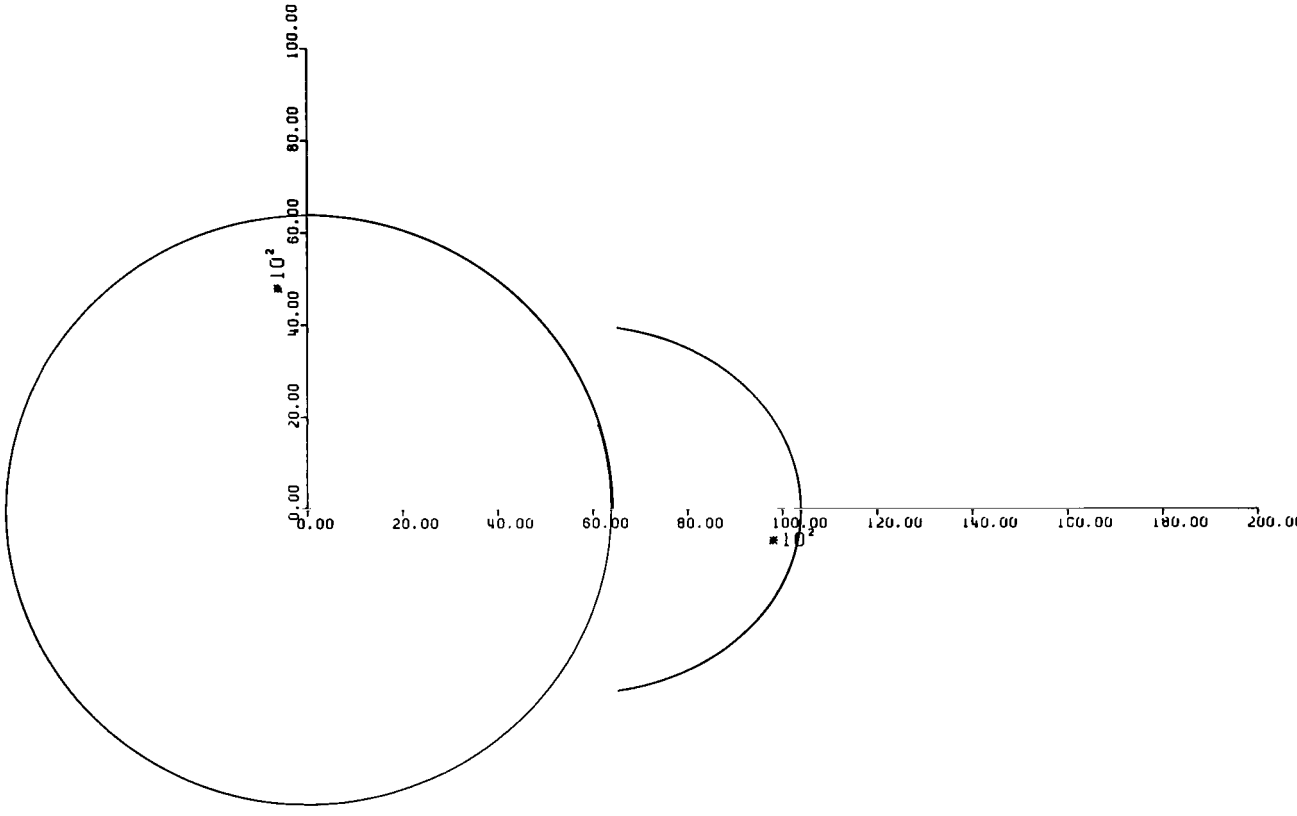

Figure 10. (Concl'd.)

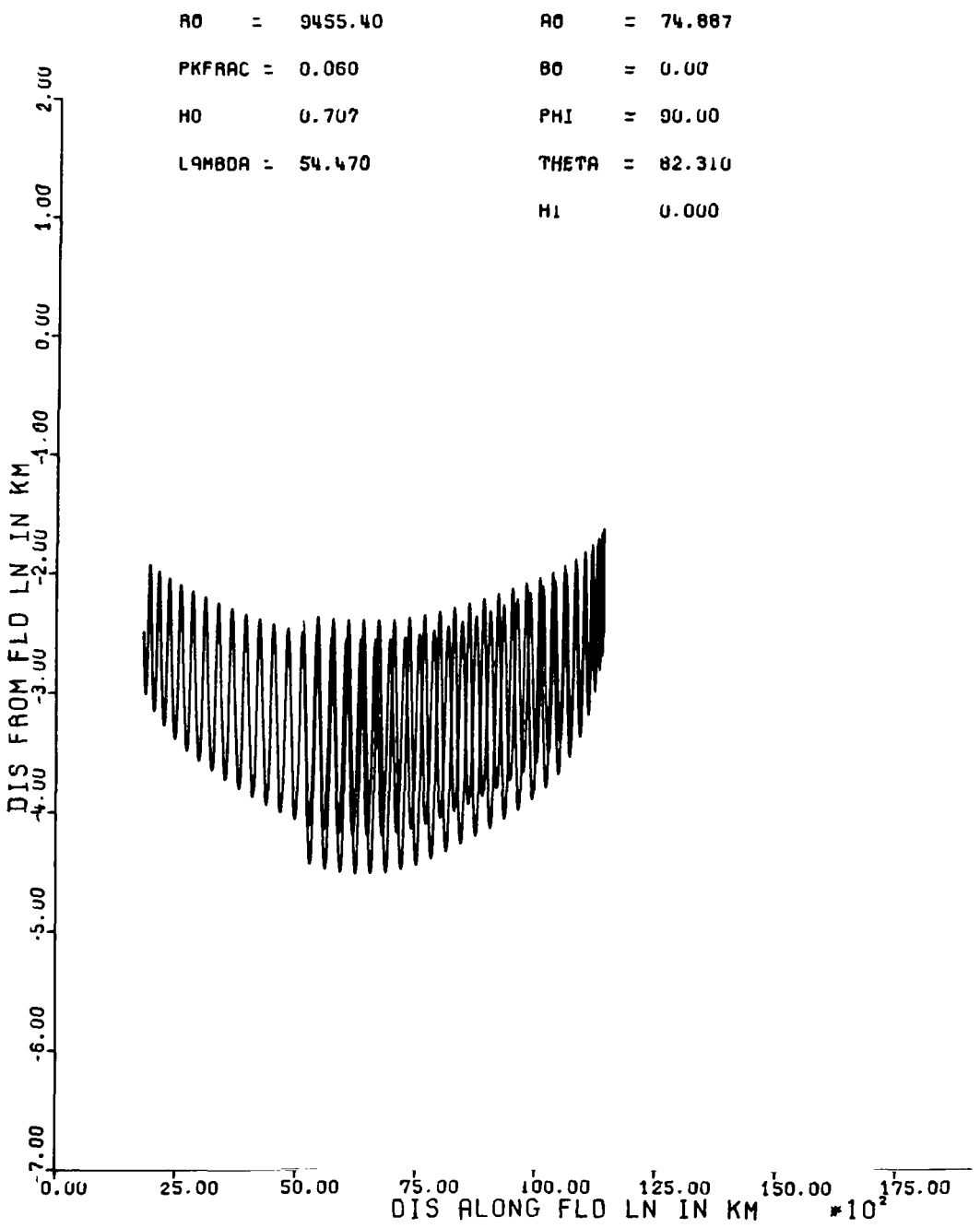

Figure 11. - Ray tracing along the L = 1.53 field line for 6.0 percent enhancement at a geocentric of 9455.50 km (frequency = 1 MHz, extraordinary wave)

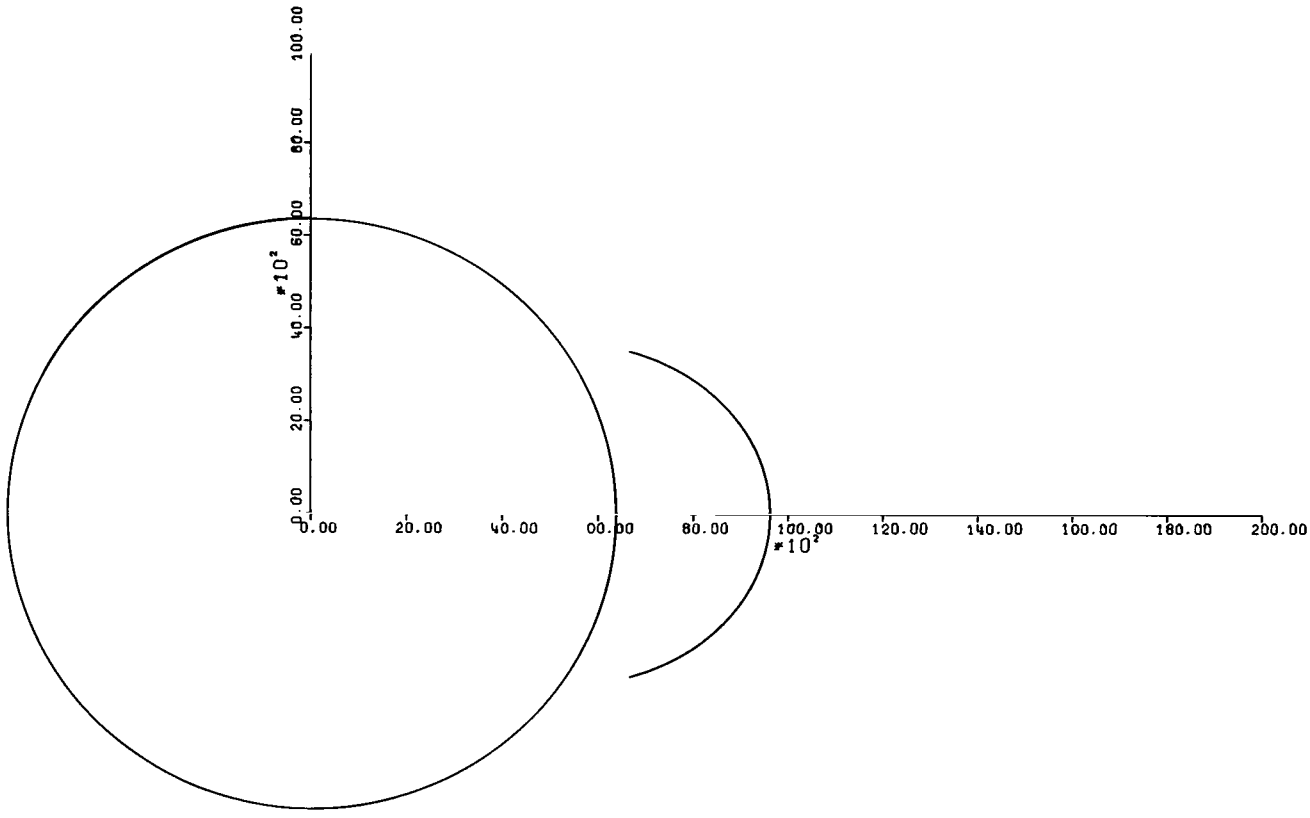

Figure 11. (Concl'd.)

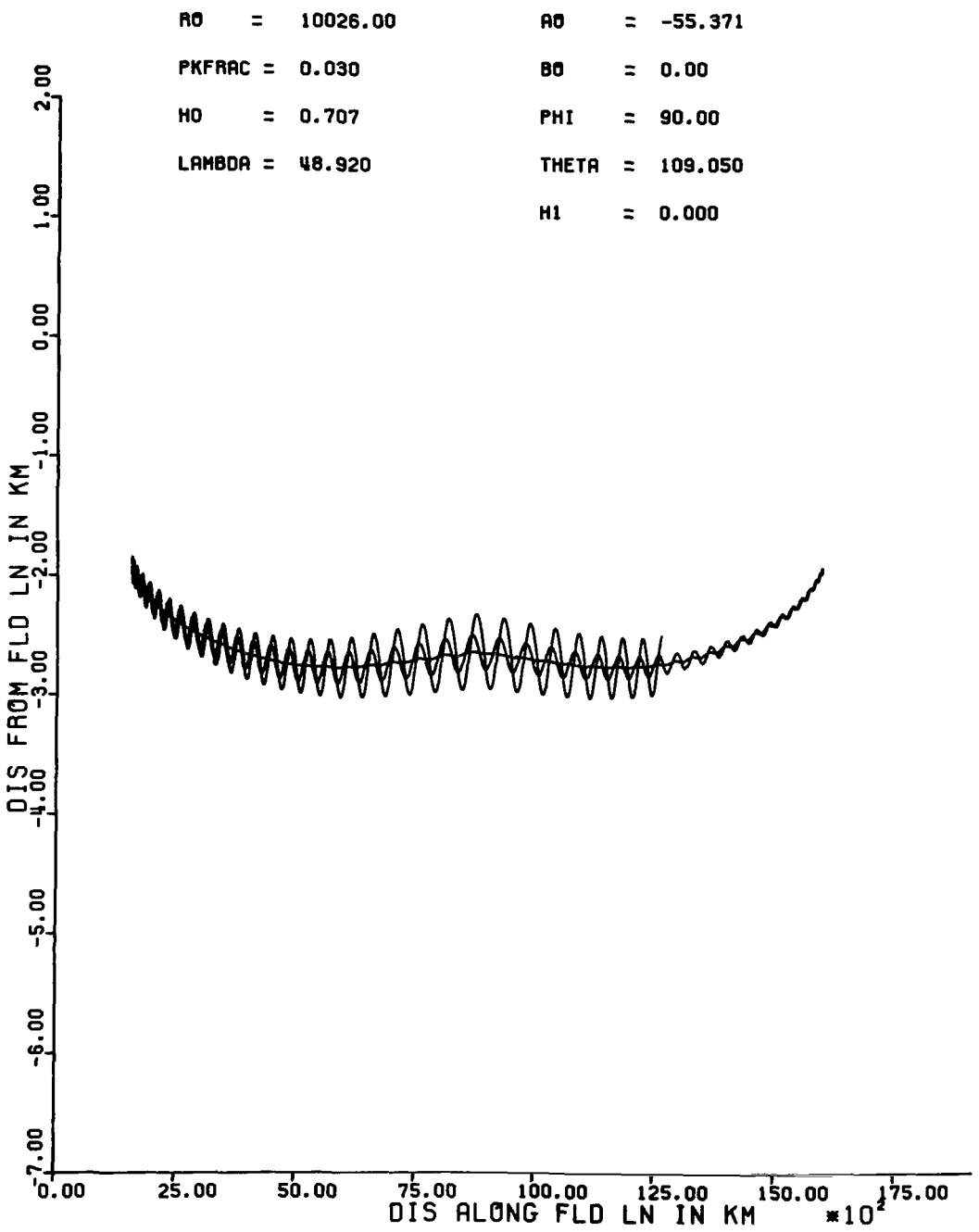

Figure 12. - Ray tracing along the L = 1.76 field line for only 3.0 percent peak enhancement of electron density at a geocentric distance of 10,026.00 km (frequency = 1 MHz)

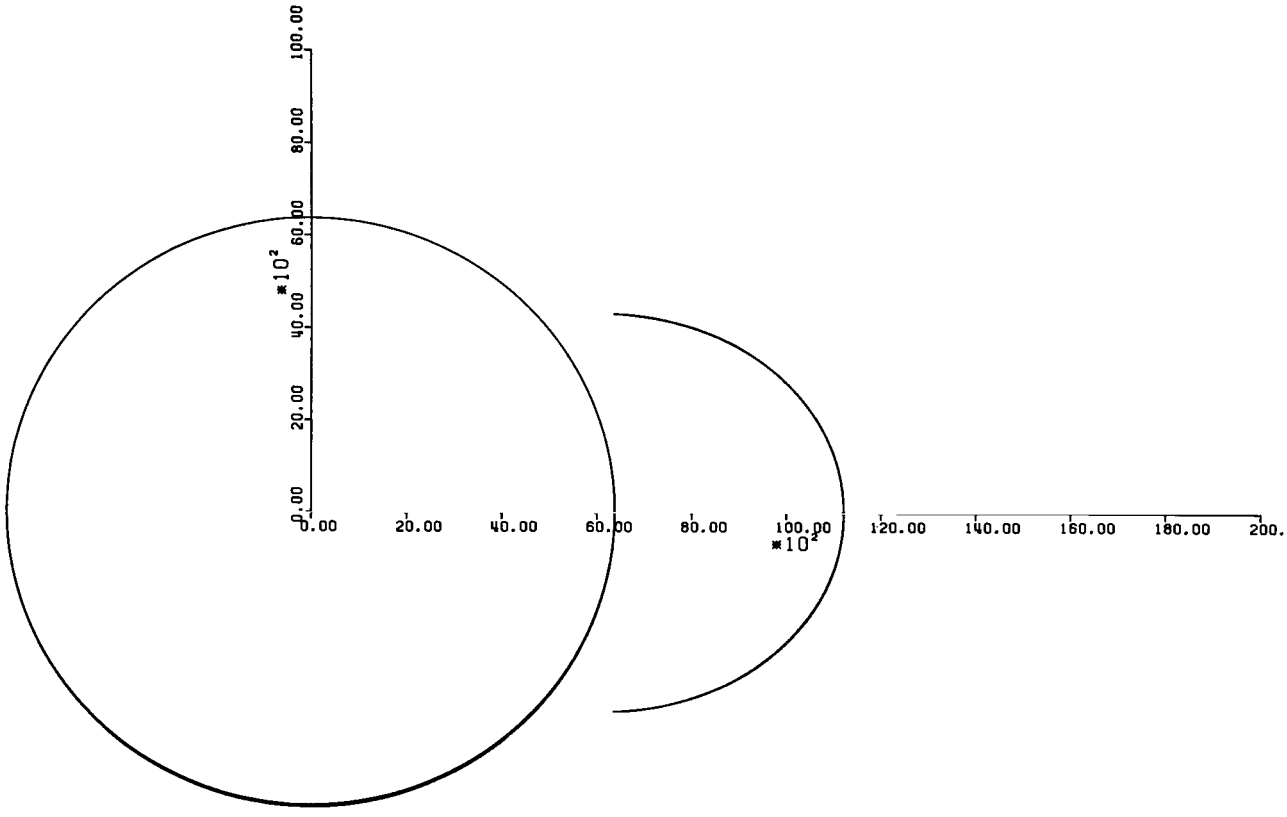

Figure 12. (Concl'd.)

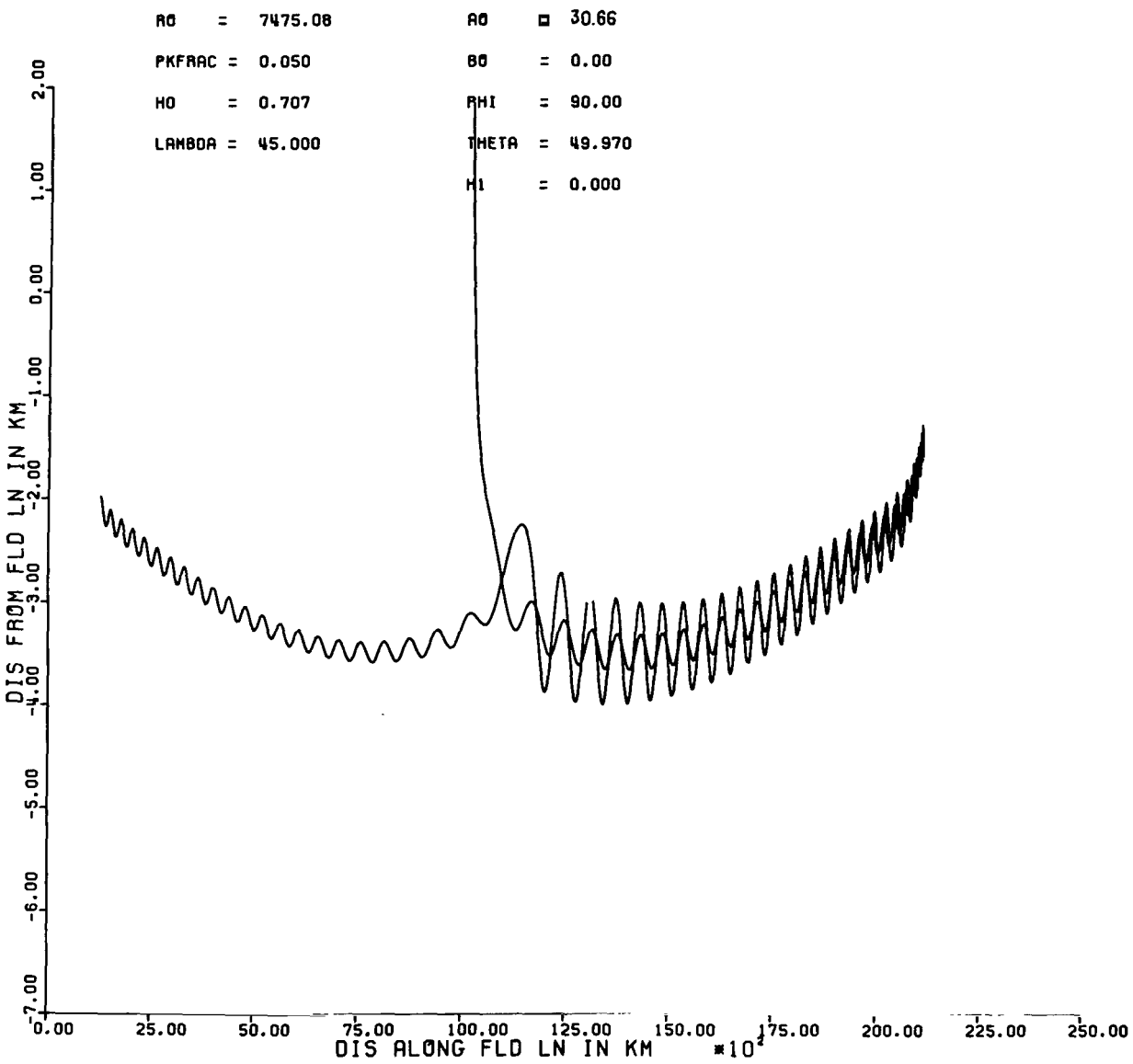

Figure 13. - Ray tracing along the L = 2.00 field line for 5.0 percent peak enhancement at a geocentric distance of 7475.08 km. (frequency = 2.0 MHz -- The ray escapes on its trip from the conjugate point)

REFERENCES

1. Muldrew, D.B.: Radio Propagation along Magnetic Field-Aligned Sheets of Ionization Observed by the Alouette-1 Topside Sounder. J. Geophys. Res., vol. 68, pp. 5355-5370, 1963.
2. Loftus, B.T., Van Zandt, T.E., and Calvert, W.: Observations of Conjugate Ducting by the Fixed-Frequency Topside-Sounder Satellite. Ann. de Geophys., vol. 22, pp. 530-537, 1966.
3. Muldrew, D.B.: MF Conjugate Echoes Observed on Alouette-2 Topside-Sounder Data. Can. J. Phys., vol. 45, no. 12, pp. 3935-3944, 1967.
4. Ramasastry, J.: Review of High-Frequency Radiowave Ducting in the Magnetosphere of the Earth, NASA TMX-1457, 1967.
5. Hamilton, W.R.: Geometrical Optics, Vol 1 of the Mathematical Papers of Sir William Rowan Hamilton. A.W. Conway and J.L. Synge, eds., Cambridge University Press, Cambridge, 1931.
6. Haselgrove, J.: Ray Theory and a New Method of Ray-Tracing, The Physics of the Ionosphere. The Physical Society, London, pp. 355-364, 1965.
7. Grossi, M.D., and Langworthy, B.M.: Geometrical Optics Investigation of HF and VHF Guided Propagation in the Ionospheric Whispering Gallery. Radio Science, vol. 1 (New Series), no. 8, pp. 877-886, 1966.
8. Barker, J.I., and Grossi, M.D.: HF and VHF Ionosphere Wave Guidance. NAECON Proc., Dayton, Ohio, 1963.
9. Cain, J.C., et al.: An Evaluation of the Main Geomagnetic Field. J. Geophys. Res., vol. 70, p. 3647, 1965.
10. Johnson, F.S.: Satellite Environment Handbook. pp. 127-131, Stanford Univ. Press, Stanford, California
11. Angerami, J.J., and Thomas, J.P.: The Distribution of Ions and Electrons in the Earth's Exosphere. J. Geophys. Res., vol. 69, pp. 4537-4560, 1964.
12. Thomas, J.O., and Sader, A.Y.: Alouette-1 Topside Soundings Monitored at Stanford University., Stanford Electronic Lab. Tech. Rept. 6, Radio Science Lab., Stanford Univ., 1963.
13. Swayzee, D.W.: Digital Ray-Tracing Investigation of HF Guided Propagation in the Magnetosphere, Tech. Memo 145, Philco-Ford Corporation, Palo Alto, California, June 1968.

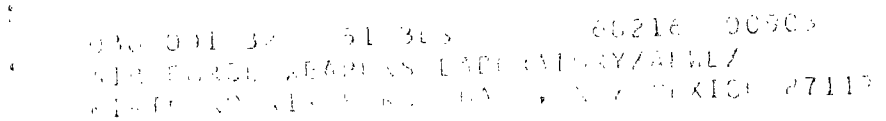

"The aeronautical and space activities of the United States shall be conducted so as to contribute . . . to the expansion of human knowledge of phenomena in the atmosphere and space. The Administration shall provide for the widest practicable and appropriate dissemination of information concerning its activities and the results thereof."

—NATIONAL AERONAUTICS AND SPACE ACT OF 1958

NASA SCIENTIFIC AND TECHNICAL PUBLICATIONS

TECHNICAL REPORTS: Scientific and technical information considered important, complete, and a lasting contribution to existing knowledge.

TECHNICAL NOTES: Information less broad in scope but nevertheless of importance as a contribution to existing knowledge.

TECHNICAL MEMORANDUMS: Information receiving limited distribution because of preliminary data, security classification, or other reasons.

CONTRACTOR REPORTS: Scientific and technical information generated under a NASA contract or grant and considered an important contribution to existing knowledge.

TECHNICAL TRANSLATIONS: Information published in a foreign language considered to merit NASA distribution in English.

SPECIAL PUBLICATIONS: Information derived from or of value to NASA activities. Publications include conference proceedings, monographs, data compilations, handbooks, sourcebooks, and special bibliographies.

TECHNOLOGY UTILIZATION PUBLICATIONS: Information on technology used by NASA that may be of particular interest in commercial and other non-aerospace applications. Publications include Tech Briefs, Technology Utilization Reports and Notes, and Technology Surveys.

Details on the availability of these publications may be obtained from:

SCIENTIFIC AND TECHNICAL INFORMATION DIVISION

NATIONAL AERONAUTICS AND SPACE ADMINISTRATION

Washington, D.C. 20546